Journal of Biomechanics 45 (2012) 2271–2278

Contents lists available at SciVerse ScienceDirect

Journal of Biomechanics

journal homepage: www.elsevier.com/locate/jbiomech
www.JBiomech.com

Muscle and prosthesis contributions to amputee walking mechanics: A modeling study

Anne K. Silverman [a,*], Richard R. Neptune [b]

[a] Department of Mechanical Engineering, Colorado School of Mines, Golden, CO 80401, USA
[b] Department of Mechanical Engineering, The University of Texas at Austin, Austin, TX 78712, USA

ARTICLE INFO

Article history:
Accepted 2 June 2012

Keywords:
Biomechanics
Transtibial
Below-knee
Forward dynamics
Simulation

ABSTRACT

Unilateral, below-knee amputees have altered gait mechanics, which can significantly affect their mobility. Below-knee amputees lose the functional use of the ankle muscles, which are critical during walking to provide body support, forward propulsion, leg-swing initiation and mediolateral balance. Thus, either muscles must compensate or the prosthesis must provide the functional tasks normally provided by the ankle muscles. Three-dimensional (3D) forward dynamics simulations of amputee and non-amputee walking were generated to identify muscle and prosthesis contributions to amputee walking mechanics, including the subtasks of body support, forward propulsion, leg-swing initiation and mediolateral balance. Results showed that the prosthesis provided body support in the absence of the ankle muscles. The prosthesis contributed to braking from early to mid-stance and propulsion in late stance. The prosthesis also functioned like the uniarticular soleus muscle by transferring energy from the residual leg to the trunk to provide trunk propulsion. The residual-leg vasti and rectus femoris reduced their contributions to braking in early stance, which mitigated braking from the prosthesis during this period. The prosthesis did not replace the function of the gastrocnemius, which normally generates energy to the leg to initiate swing. As a result, lower overall energy was delivered to the residual leg. The prosthesis also acted to accelerate the body laterally in the absence of the ankle muscles. These results provide further insight into muscle and prosthesis function in below-knee amputee walking and can help guide rehabilitation methods and device designs to improve amputee mobility.

1. Introduction

Unilateral, below-knee amputee gait is characterized by bilateral asymmetry, leg and back pain and a reduced self-selected walking speed compared to non-amputee walking (for review, see Hafner et al., 2002; Kulkarni et al., 2005). These abnormal gait characteristics are largely the result of the functional loss of the residual-leg ankle plantarflexors, which are critical for providing body support, forward propulsion, leg-swing initiation and mediolateral balance in non-amputee walking (e.g., Liu et al., 2006; Neptune et al., 2001, 2004; Pandy et al., 2010; Zajac et al., 2003). As a result, either muscles must compensate or the prosthesis must provide these important functional tasks normally provided by the ankle muscles.

Experimental studies have identified a number of compensations in amputee walking through analysis of ground reaction force (GRF), joint kinetic and muscle electromyography (EMG) data. Studies have shown that amputees have greater dependence on the intact leg through increased GRFs relative to the residual leg (e.g., Arya et al., 1995; Nolan et al., 2003; Sanderson and Martin, 1997). Both the residual and intact legs have greater hip extensor moments and do more work in early stance relative to non-amputees (Gitter et al., 1991; Grumillier et al., 2008; Silverman et al., 2008). In addition, amputees often generate higher residual leg hip flexor moments and power in pre-swing compared to non-amputees (Sadeghi et al., 2001). EMG studies have shown prolonged residual-leg muscle activity in the vasti and hamstring muscles relative to the intact leg (Fey et al., 2010; Isakov et al., 2001; Pinzur et al., 1991) and non-amputees (Powers et al., 1998; Winter and Sienko, 1988). Prolonged intact-leg gluteus maximus activity relative to non-amputees has also been observed (Culham et al., 1986; Torburn et al., 1990; Winter and Sienko, 1988). These studies highlight the range of compensatory mechanisms used in amputee walking. However, it is unclear how individual muscles involved in these compensatory mechanisms, as well as passive prostheses, contribute to specific walking subtasks of body support, forward propulsion, leg-swing initiation and mediolateral balance.

* Corresponding author. Tel.: +1 303 384 2162; fax: +1 303 273 3602.
E-mail address: asilverm@mines.edu (A.K. Silverman).

0021-9290/$ - see front matter © 2012 Elsevier Ltd. All rights reserved.
http://dx.doi.org/10.1016/j.jbiomech.2012.06.008

Previous studies investigating muscle contributions to these walking subtasks have primarily focused on non-amputees. However, one modeling study identified the muscle compensations necessary for an amputee model to walk with a symmetric, non-amputee walking pattern (Zmitrewicz et al., 2007). Compared to a non-amputee model, power output from hip flexors to accelerate the residual leg into swing increased in the amputee model. The residual-leg rectus femoris and intact-leg rectus femoris and soleus all transferred more energy from the leg to the trunk to propel it forward compared to the non-amputee model. In addition, the prosthesis functioned like the uniarticular soleus by absorbing energy from the leg and delivering it to the trunk, although the energy it returned was only a portion of the normal soleus output. While this analysis provided insight into potential muscle compensatory mechanisms needed to produce a symmetric gait pattern, the simulation did not reflect realistic amputee gait mechanics and was limited to the sagittal plane. Analyzing 3D amputee walking mechanics is an important next step because amputee gait is characterized by asymmetric joint kinematics and kinetics and GRFs in all three planes (e.g., Hafner et al., 2002; Royer and Wasilewski, 2006; Underwood et al., 2004), which may influence needed muscle compensations.

Therefore, the objective of this study was to develop 3D forward dynamics simulations of both amputee and non-amputee walking to determine how the prosthesis and individual muscles work in synergy to provide body support, forward propulsion, leg-swing initiation and mediolateral balance during amputee walking.

2. Methods

2.1. Musculoskeletal model

A 3D, bipedal musculoskeletal model was developed using SIMM/Dynamics Pipeline (Musculographics, Inc.) and has been previously described in detail (Peterson et al., 2010). The dynamic equations-of-motion were generated using SD/FAST (PTC). The model consisted of 14 rigid body segments including a head-arms-trunk (HAT) segment, pelvis and two legs. Each leg consisted of segments for the thigh, shank, patella, talus, calcaneus and toes. The model had a total of 23 degrees-of-freedom. A six degree-of-freedom joint was defined between the ground and pelvis. The HAT and each thigh had three rotational degrees-of-freedom with respect to the pelvis. There was one rotational degree-of-freedom defined at the knee, ankle, subtalar and metatarsalphalangeal joints. Each leg was driven by 38 Hill-type musculotendon actuators governed by intrinsic force–length–velocity relationships (Zajac, 1989, Table 1), with musculoskeletal geometry based on Delp et al. (1990). The excitation for each muscle was defined using a bimodal excitation pattern defined as

$$u(t)=\sum_{i=1}^{2}\begin{cases}\text{if } onset_i \le t \le offset_i\\ \frac{A_i}{2}\left[1-\cos\left(2\pi\cdot\frac{t-onset_i}{offset_i-onset_i}\right)\right]\\ \text{else}\\ 0\end{cases} \quad (1)$$

where $u(t)$ is the excitation of a muscle at time t. A_i, $onset_i$ and $offset_i$ were the amplitude, onset and offset of mode i. The bimodal onsets, offsets and magnitudes were optimized, resulting in six optimization parameters per muscle. For the non-amputee model, symmetric excitation patterns were used between legs to reduce the number of optimization parameters and also because the corresponding experimental kinematics and kinetics were nearly symmetrical.

Muscle activation/deactivation dynamics were modeled using a first-order differential equation (Raasch et al., 1997), with activation and deactivation time constants from Winters and Stark (1988). Foot-ground contact was modeled using 31, independent visco-elastic elements with coulomb friction on each foot (Neptune et al., 2000). Passive torques were applied at each joint to represent ligament and passive tissue forces (Anderson and Pandy, 1999; Anderson, 1999; Davy and Audu, 1987).

For the amputee model, the residual shank mass was half of the intact shank, and the residual shank center-of-mass location was moved proximally such that it was 25% of the total knee-to-ankle distance distal from the knee. Seven residual leg muscles crossing the ankle joint were removed (Table 1). The prosthesis was modeled to replicate experimentally measured ankle torque values derived with inverse dynamics using a second-order torsional spring with damping as

$$\tau = a_0 + a_1\theta + a_2\dot{\theta} + a_3\theta^2 + a_4\theta\dot{\theta} \quad (2)$$

Table 1
Muscles included in the model and corresponding muscle groups. Shaded muscles were not included in the residual leg of the amputee model.

Muscle	Muscle group
Iliacus Psoas	IL
Adductor longus Adductor brevis Pectineus Quadratus femoris	AL
Adductor magnus (superior, middle, and inferior compartments)	AM
Sartorius	SAR
Rectus femoris[a]	RF
Vastus medialis Vastus intermedius Vastus lateralis[a]	VAS
Gluteus medius (anterior and middle compartments)[a] Gluteus minimus (anterior and middle compartments)	GMEDA
Gluteus medius (posterior compartment) Gluteus minimus (posterior compartment) Gemellus Piriformis	GMEDP
Tensor fascia lata	TFL
Gluteus maximus (superior, middle and inferior compartments)[a]	GMAX
Semimembranosus Semitendinosus Gracilis Biceps femoris long head[a]	HAM
Biceps femoris short head	BFSH
Gastrocnemius (medial and lateral heads)[a]	GAS
Soleus[a] Tibialis posterior Flexor digitorum longus	SOL
Tibialis anterior[a] Extensor digitorum longus	TA

[a] EMG data were available for muscles.

where θ is the ankle angle, $\dot{\theta}$ is the ankle velocity, τ is the prosthesis torque, and a_0 through a_4 are constant coefficients determined by fitting Eq. (2) to the average amputee experimental torque and kinematic data (see Experimental Data Collection section). The coefficients were determined using a multiple regression analysis of the experimental data to estimate the prosthesis torque using the ankle angle and velocity as inputs.

2.2. Optimization framework

A simulated annealing optimization algorithm (Goffe et al., 1994) was used to solve the optimal tracking problem to generate three forward dynamics simulations (Fig. 1). The simulations consisted of the amputee residual leg stance, amputee intact leg stance and non-amputee left leg stance. The optimization cost function consisted of the difference between the average experimental and simulated joint kinematics and GRFs as

$$J=\sum_{j=1}^{m}\sum_{i=1}^{n}\frac{(Y_{ij}-\hat{Y}_{ij})^2}{SD_{ij}^2} \quad (3)$$

where Y_{ij} is the experimental measurement of variable j at time step i, $\hat{Y}_{ij}$ is the corresponding simulation value, and SD_{ij}^2 is the average experimental variability of variable j across trials. The optimization algorithm modified the timing and magnitude of the muscle excitation patterns to minimize Eq. (3).

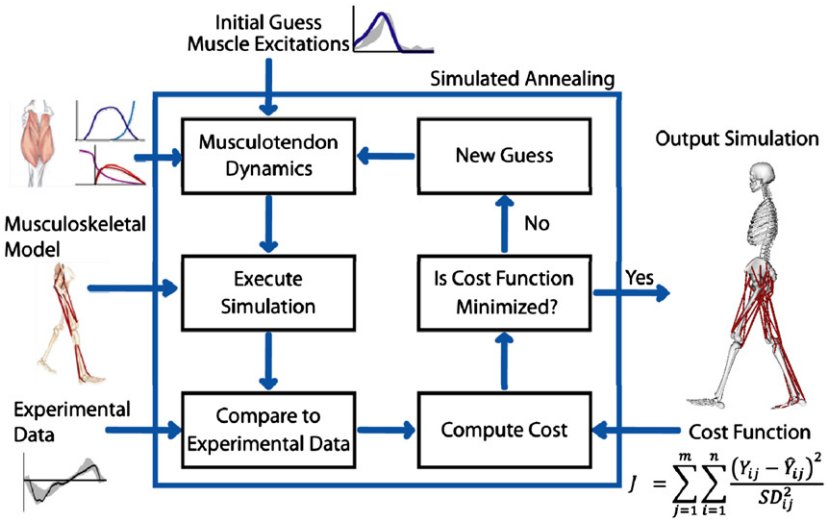

Fig. 1. Dynamic optimization framework used to generate the amputee and non-amputee simulations. An initial guess for the muscle excitations was provided from the EMG data and musculotendon dynamics were used to determine the corresponding muscle forces. The muscle forces were applied to the musculoskeletal model and the simulation was executed by integrating the equations-of-motion. The simulated motion was compared to the experimental data and the optimization cost function was computed. The optimization algorithm then fine-tuned the muscle excitations until the output from the simulation reproduced the experimental data (i.e., the cost function was minimized).

Table 2
Mean (SD) subject characteristics for the amputees and non-amputees. Time from amputation, prosthetic foot type and etiology are reported for the amputees. The prosthetic foot type is classified as energy storage and return (ESAR) or solid ankle cushioned heel (SACH).

	Age (years)	Body mass (kg)	Body height (m)	Time since amputation (years)	Foot type	Etiology
Amputees	45.1 (9.1)	90.5 (18.6)	1.75 (0.10)	5.6 (2.9)	9 ESAR/ 5 SACH	11 Traumatic/3 vascular
Non-amputees	34.1 (13.0)	70.9 (13.6)	1.76 (0.11)	–	–	–

2.3. Assessing muscle and prosthesis function

Muscle and prosthesis function was determined using a previously described GRF decomposition, and induced acceleration and segment power analyses (Fregly and Zajac, 1996; Neptune et al., 2001). For the analyses, muscles were combined into 15 muscle groups based on muscle function and anatomical classification (Table 1). The contributions of the prosthesis and individual muscles to body support, forward propulsion and mediolateral balance were quantified by their contributions to the vertical, horizontal and mediolateral GRFs, respectively. Contributions to propulsion were further investigated by examining trunk (sum of the pelvis and HAT segments) propulsion and leg-swing initiation. Trunk propulsion was quantified as the horizontal power delivered to the trunk. Leg-swing initiation was quantified by the energy delivered to the leg during the second double support (pre-swing) phase. Muscle and prosthesis contributions were compared between the residual, intact and non-amputee legs during the respective stance phases to identify compensatory mechanisms.

2.4. Experimental data collection

The experimental data collection methods have been previously described in detail (Fey et al., 2010; Silverman et al., 2008) and are presented briefly here. Fourteen amputees and 10 non-amputees (Table 2) walked overground at 1.2 ± 0.06 m/s. All subjects provided informed consent to an Institutional Review Board approved protocol. 3D kinematic data were collected at 120 Hz, and GRF and EMG data were collected at 1200 Hz. A minimum of five force-plate hits per leg were collected. EMG data were collected using surface electrodes from eight intact-leg muscles and five residual-leg muscles (Table 1). Each amputee subject used his or her own prosthesis.

Kinematic and GRF data were low-pass filtered using a fourth-order Butterworth filter with a cutoff frequency of 6 Hz and 20 Hz, respectively. EMG data were demeaned, rectified, high-pass filtered with a cutoff frequency of 40 Hz, and then low-pass filtered with a cutoff frequency of 4 Hz. Data were normalized to the gait cycle and averaged across subjects for both the amputee and non-amputee groups.

3. Results

The simulated kinematics and kinetics reproduced the experimental walking data, with the differences between the simulation and experimental average less than two standard deviations (2 SD) of the experimental data for all three simulations. Thus, the simulations were statistically indistinguishable from the average experimental data. The residual leg stance simulation had an average kinematic difference of 4.01° (2 SD = 10.54°), GRF difference of 5.24 % body weight (2 SD = 5.35 %BW), joint moment difference of 0.151 Nm/kg (2 SD = 0.236 Nm/kg) and joint power difference of 0.204 W/kg (2 SD = 0.418 W/kg) from the experimental data. Similarly, the intact leg stance simulation had average differences of 4.73°, 4.42 %BW, 0.144 Nm/kg and 0.201 W/kg (2 SD = 10.41°, 5.32 %BW, 0.216 Nm/kg and 0.347 W/kg) and the non-amputee left leg stance simulation had average differences of 4.87°, 5.09 %BW, 0.116 Nm/kg and 0.271 W/kg (2 SD = 10.82°, 6.07 %BW, 0.229 Nm/kg and 0.283 W/kg). In addition, the optimized excitation patterns qualitatively agreed well with the experimental EMG data.

3.1. Body support

Primary muscle contributors to body support in early stance in all three legs were VAS, GMAX, GMEDA and GMEDP (Fig. 2). In the second half of stance, the prosthesis provided the majority of the support in the residual leg while the plantarflexors provided support in the intact and non-amputee legs.

3.2. Body propulsion

The primary contributors to body propulsion were similar in all three legs, although the relative magnitude of the contributions varied across legs. In early stance, VAS and RF contributed to braking (negative body propulsion) and HAM contributed to body propulsion in all three legs (Fig. 3). The braking contributions from VAS and RF were smaller in the residual leg compared to the

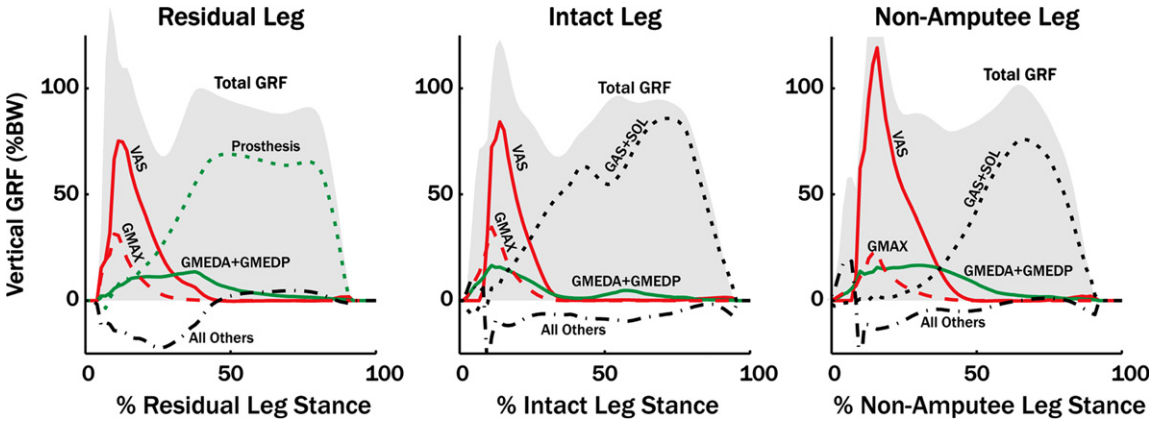

Fig. 2. Ipsilateral leg muscle group contributions to the vertical ground reaction force (GRF).

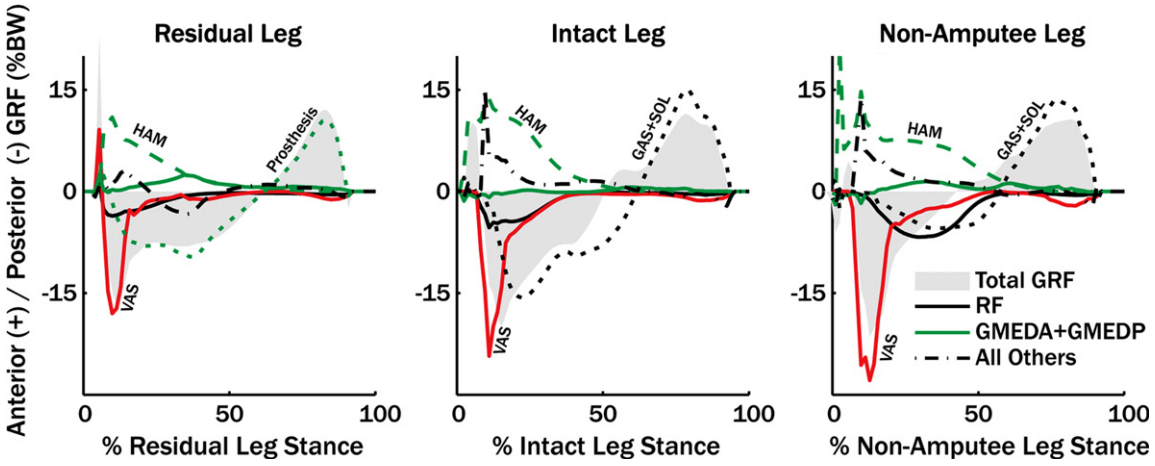

Fig. 3. Ipsilateral leg muscle group contributions to the anterior/posterior (A/P) ground reaction force (GRF).

non-amputee leg. The gluteus medius also contributed to body propulsion in early to mid-stance in all three legs. The prosthesis contributed to braking in early stance and propulsion in late stance. SOL and GAS contributed to braking in early to mid-stance and then propulsion in late stance in both the non-amputee and intact legs.

3.3. Trunk propulsion

VAS, RF and SOL were the primary contributors to positive net trunk power in the non-amputee leg, which was similar to the intact leg (Fig. 4). Specifically, these muscles all contributed to horizontal trunk power in the intact and non-amputee legs, providing trunk propulsion (Fig. 5). In the residual leg, VAS, RF and the prosthesis were the largest contributors to positive net trunk power (Fig. 4), which provided trunk propulsion (Fig. 5).

3.4. Leg-swing initiation

In pre-swing, IL, AL, SAR and GAS delivered energy to the ipsilateral leg in the non-amputee and intact legs for swing initiation (Fig. 6). IL, AL and SAR were also major contributors to swing initiation in the residual leg. The prosthesis absorbed energy from the residual leg throughout stance, and delivered a small amount of energy to the leg during the pre-swing phase, with a net negative contribution over the pre-swing phase (Figs. 4, 6 and 7). In addition, the residual leg muscles did not generate as much total energy to the leg over the pre-swing phase compared to the non-amputee leg.

3.5. Mediolateral balance

In all three legs, GMEDA, GMEDP and TFL were the largest contributors to the medial GRF (Fig. 8). SAR also contributed medially in all three legs, but had a much greater contribution in the residual leg. The adductors contributed laterally throughout stance and HAM contributed laterally from early to mid-stance. In the non-amputee leg, VAS contributed laterally in early stance whereas SOL and GAS contributed laterally from mid to late stance. Conversely, in the intact leg, VAS, SOL and GAS contributed medially. In the residual leg, the prosthesis contributed laterally.

4. Discussion

The purpose of this study was to determine how the prosthesis and individual muscles work in synergy to provide body support, forward propulsion, leg-swing initiation and mediolateral balance during amputee walking using forward dynamics simulation techniques. The prosthesis was found to provide substantial body support throughout residual leg stance, which was consistent with a previous 2D amputee symmetric walking simulation that showed the prosthesis provides needed support in the absence of the ankle muscles (Zmitrewicz et al., 2007). VAS, GMED and GMAX also provided body support in early stance in all three legs, which is in agreement with previous non-amputee simulation studies (Anderson and Pandy, 2003; Liu et al., 2006; Neptune et al., 2004).

While the prosthesis provided body support, it also contributed to braking from early to mid-stance (Fig. 3). The simulation results

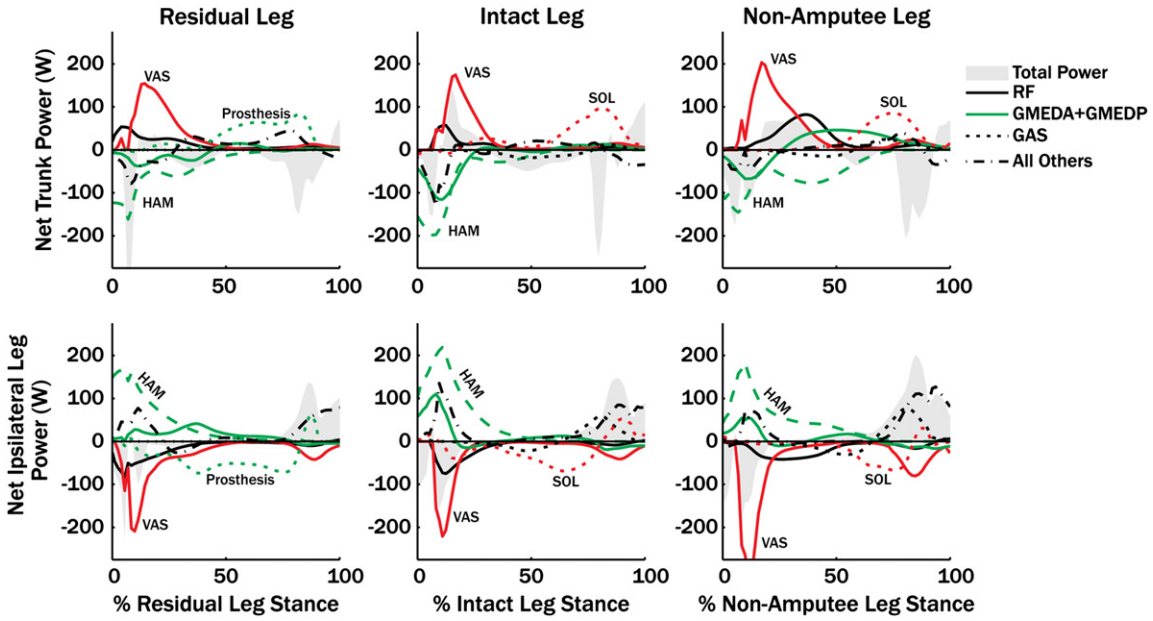

Fig. 4. Ipsilateral leg muscle group contributions to the net trunk (pelvis+HAT) and ipsilateral leg power. The shaded area is the net power (i.e., time rate of change of the kinetic and potential energy) for the trunk and leg.

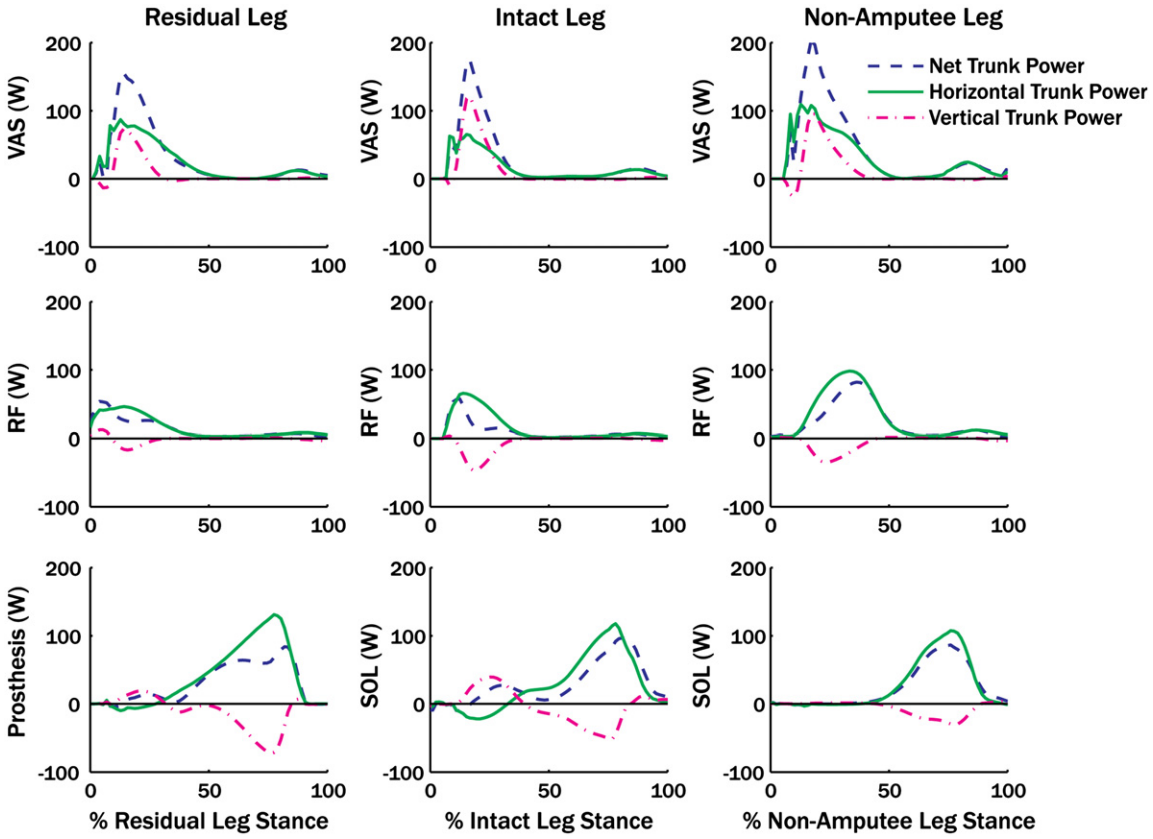

Fig. 5. Net trunk (pelvis+HAT segments) mechanical power from VAS, RF, SOL and the prosthesis. Horizontal (solid line) and vertical (dashed–dotted line) components of the power are shown. Horizontal power is the time rate of change of kinetic energy in the A/P direction. Vertical power is the time rate of change of kinetic and potential energy in the vertical direction. Net power (dashed line) is the sum of the horizontal, vertical, medial/lateral and 3D rotational power components.

indicated that the prosthesis absorbed energy from the residual leg throughout stance and delivered some of that energy to the trunk (Figs. 4 and 7). The prosthesis functioned similarly to the non-amputee SOL, which also absorbed energy from the leg and delivered it to the trunk (Fig. 7). However, SOL had a greater positive contribution to body propulsion in late stance (Fig. 3). Also like SOL, the prosthesis delivered substantial horizontal power to the trunk for forward propulsion (Fig. 5). Thus, the simulation results suggest that the prosthesis was able to partially compensate for the ankle plantarflexors to provide trunk propulsion through elastic energy storage and return, but at the expense of absorbing more energy from the leg and reducing overall body propulsion.

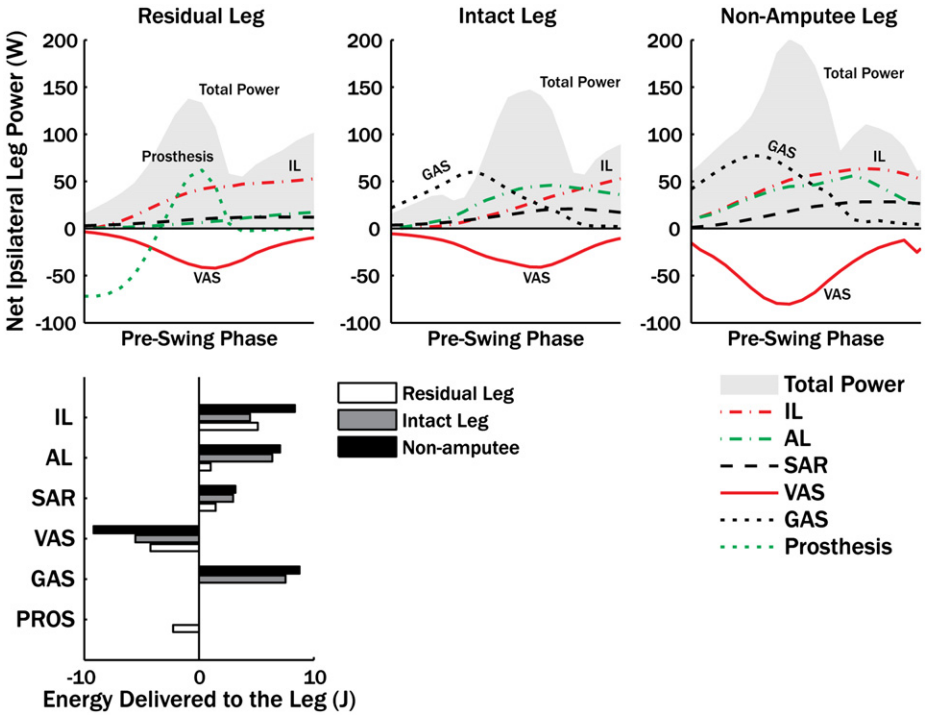

Fig. 6. Muscle group contributions to the net ipsilateral leg power during the pre-swing phase in each simulation. Total mechanical energy delivered to the leg from individual muscle groups during the pre-swing phase is also shown.

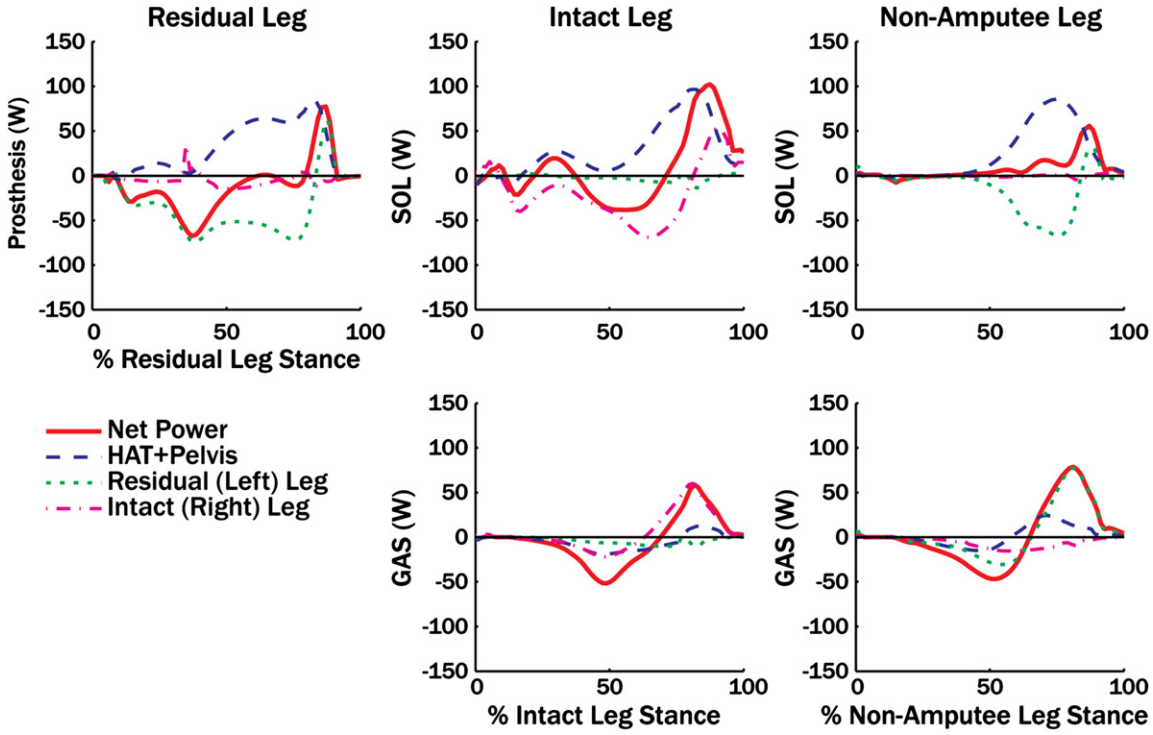

Fig. 7. Net musculotendon power distributed to the legs and trunk (pelvis+HAT segments) for the GAS and SOL groups in the non-amputee and intact leg simulations compared to the prosthesis in the residual leg simulation.

The prosthesis returned some energy to the leg immediately prior to swing. However, the net energy delivered to the leg from the prosthesis was negative over pre-swing (Fig. 6), and therefore the prosthesis did not return enough energy to the leg to replace the function normally provided by GAS (Figs. 6 and 7).

The mediolateral simulation results for the non-amputee and residual legs were consistent with previous non-amputee walking studies, with the gluteus medius contributing to the medial GRF, and the adductors, SOL, GAS, VAS and HAM contributing to the lateral GRF (Pandy et al., 2010; Fig. 8). However, the residual leg

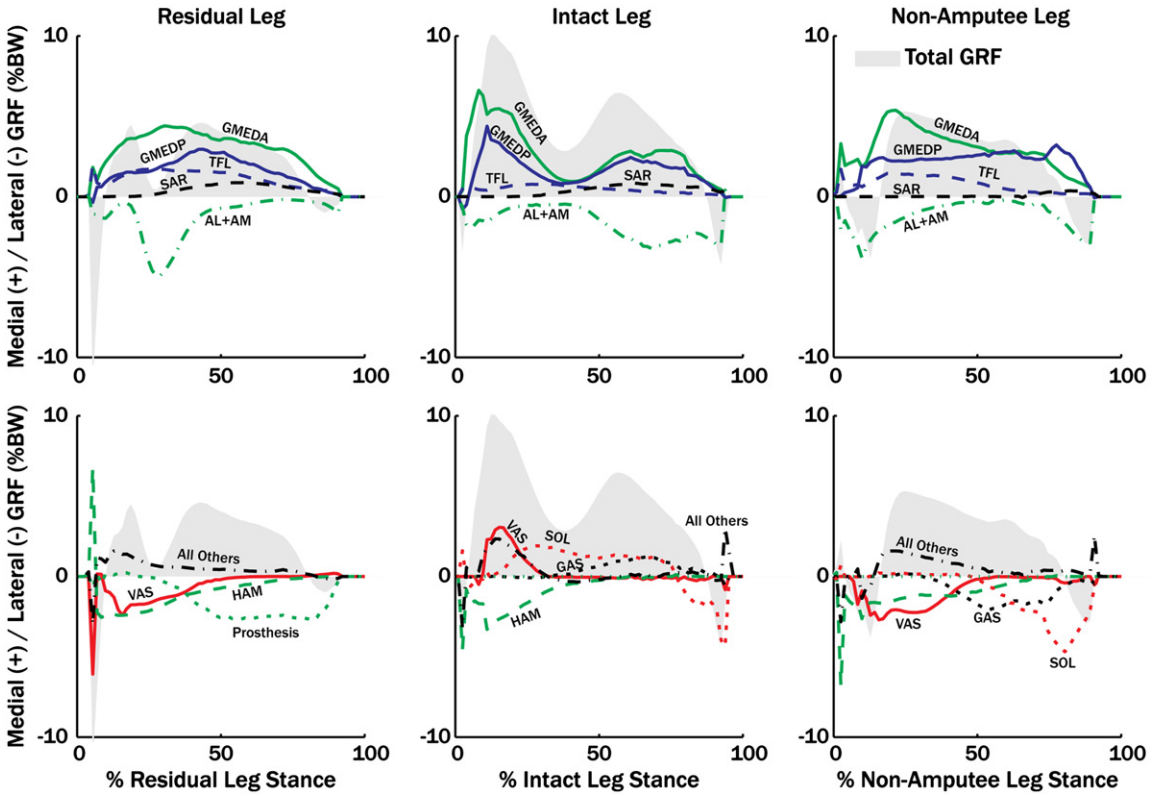

Fig. 8. Ipsilateral leg muscle group contributions to the mediolateral ground reaction force (GRF).

had greater medial contributions from SAR and lateral contributions from the prosthesis in the absence of the plantarflexors. The intact leg results were different, with VAS, GAS and SOL contributing medially. The different results arise from a larger step width in the intact leg simulation, with the intact hip remaining abducted through the majority of stance. The intact leg had 5.7° average and 9.2° maximum hip abduction, compared to 1.0° average and 4.3° maximum for the non-amputee leg. Knee and ankle extension generated by VAS, GAS and SOL acted to push the foot laterally against the ground, resulting in a medial GRF. This result highlights importance of foot placement relative to the body center-of-mass to control mediolateral balance.

While the results indicated that the prosthesis provided sufficient body support and lateral acceleration, body propulsion and leg-swing initiation were reduced in the absence of the ankle plantarflexors. The largest differences between the amputee and non-amputee simulations were in VAS and RF. Both VAS and RF acted to transfer energy from the leg to the trunk, consistent with previous non-amputee simulation results (Neptune et al., 2004). Both muscles provided trunk propulsion while braking the body center-of-mass (Figs. 3–5). In the residual leg, the braking contributions from VAS and RF were reduced relative to the intact and non-amputee legs. This result is consistent with previous studies showing atrophy in the residual leg thigh muscles (Moirenfeld et al., 2000; Renstrom et al., 1983), which leads to a smaller force output from these muscles. Reduced contributions from VAS and RF mitigated braking from the prosthesis in early to mid-stance.

Although this study identified important compensatory mechanisms needed for amputee walking, a potential limitation to this study is that group average amputee data were simulated. Experimental studies have shown that amputees have a wide variety of individual compensatory mechanisms (e.g., Silverman et al., 2008), some of which may not be apparent in the amputee average data. Thus, future work should be directed at analyzing subject-specific simulations to identify other muscle compensatory mechanisms that can help tailor rehabilitation methods to an individual. In addition, the present study analyzed walking at a nominal speed, which is applicable to understanding overall amputee walking mechanics. However, certain deficits and compensatory mechanisms used in amputee gait are more prominent at faster walking speeds (Nolan et al., 2003; Sanderson and Martin, 1997; Silverman et al., 2008), and therefore additional muscle compensations may be necessary to achieve faster walking speeds.

5. Conclusion

The results of this study showed that in the absence of the ankle muscles, the prosthesis provided needed body support and lateral acceleration. The prosthesis acted to absorb energy from the residual leg and transfer some of that energy to the trunk. Reduced braking contributions from the residual leg vasti and rectus femoris mitigated additional braking from the prosthesis. The prosthesis did not provide as much energy to the leg for swing initiation compared to the non-amputee gastrocnemius. Thus, the total energy of the residual leg during the pre-swing phase was lower compared to the non-amputee leg. These results are important for understanding functional deficits in amputee gait, as well as designing future assistive devices and rehabilitation strategies. Currently, the prosthesis provides body support, lateral acceleration and trunk propulsion. However, devices that provide additional body propulsion and leg-swing initiation could augment current function. In addition, rehabilitation methods may be used to train other muscles, such as the iliopsoas, to compensate for the gastrocnemius and increase the energy delivered to the leg for swing initiation.

Conflict of interest statement

None.

Acknowledgments

This work was supported by the National Science Foundation, Grant no. 0346514.

References

Anderson, F.C., 1999. A dynamic optimization solution for a complete cycle of normal gait. Ph.D. Thesis. The University of Texas at Austin.

Anderson, F.C., Pandy, M.G., 1999. A dynamic optimization solution for vertical jumping in three dimensions. Computer Methods in Biomechanics and Biomechanical Engineering 2, 201–231.

Anderson, F.C., Pandy, M.G., 2003. Individual muscle contributions to support in normal walking. Gait & Posture 17, 159–169.

Arya, A., Lees, A., Nerula, H., Klenerman, L., 1995. A biomechanical comparison of the SACH, Seattle and Jaipur feet using ground reaction forces. Prosthetics and Orthotics International 19, 37–45.

Culham, E.G., Peat, M., Newell, E., 1986. Below-knee amputation: a comparison of the effect of the SACH foot and single axis foot on electromyographic patterns during locomotion. Prosthetics and Orthotics International 10, 15–22.

Davy, D.T., Audu, M.L., 1987. A dynamic optimization technique for predicting muscle forces in the swing phase of gait. Journal of Biomechanics 20, 187–201.

Delp, S.L., Loan, J.P., Hoy, M.G., Zajac, F.E., Topp, E.L., Rosen, J.M., 1990. An interactive graphics-based model of the lower extremity to study orthopaedic surgical procedures. IEEE Transactions on Biomedical Engineering 37, 757–767.

Fey, N.P., Silverman, A.K., Neptune, R.R., 2010. The influence of increasing steady-state walking speed on muscle activity in below-knee amputees. Journal of Electromyography and Kinesiology 20, 155–161.

Fregly, B.J., Zajac, F.E., 1996. A state-space analysis of mechanical energy generation, absorption, and transfer during pedaling. Journal of Biomechanics 29, 81–90.

Gitter, A., Czerniecki, J.M., DeGroot, D.M., 1991. Biomechanical analysis of the influence of prosthetic feet on below-knee amputee walking. American Journal of Physical Medicine and Rehabilitation 70, 142–148.

Goffe, W.L., Ferrier, G.D., Rogers, J., 1994. Global optimization of statistical functions with simulated annealing. Journal of Econometrics 60, 65–99.

Grumillier, C., Martinet, N., Paysant, J., Andre, J.M., Beyaert, C., 2008. Compensatory mechanism involving the hip joint of the intact limb during gait in unilateral trans-tibial amputees. Journal of Biomechanics 41, 2926–2931.

Hafner, B.J., Sanders, J.E., Czerniecki, J., Fergason, J., 2002. Energy storage and return prostheses: does patient perception correlate with biomechanical analysis? Clinical Biomechanics 17, 325–344.

Isakov, E., Burger, H., Krajnik, J., Gregoric, M., Marincek, C., 2001. Knee muscle activity during ambulation of trans-tibial amputees. Journal of Rehabilitation Medicine 33, 196–199.

Kulkarni, J., Gaine, W.J., Buckley, J.G., Rankine, J.J., Adams, J., 2005. Chronic low back pain in traumatic lower limb amputees. Clinical Rehabilitation 19, 81–86.

Liu, M.Q., Anderson, F.C., Pandy, M.G., Delp, S.L., 2006. Muscles that support the body also modulate forward progression during walking. Journal of Biomechanics 39, 2623–2630.

Moirenfeld, I., Ayalon, M., Ben-Sira, D., Isakov, E., 2000. Isokinetic strength and endurance of the knee extensors and flexors in trans-tibial amputees. Prosthetics and Orthotics International 24, 221–225.

Neptune, R.R., Kautz, S.A., Zajac, F.E., 2001. Contributions of the individual ankle plantar flexors to support, forward progression and swing initiation during walking. Journal of Biomechanics 34, 1387–1398.

Neptune, R.R., Wright, I.C., Bogert, A.J., 2000. A method for numerical simulation of single limb ground contact events: application to heel-toe running. Computer Methods in Biomechanics and Biomedical Engineering 3, 321–334.

Neptune, R.R., Zajac, F.E., Kautz, S.A., 2004. Muscle force redistributes segmental power for body progression during walking. Gait & Posture 19, 194–205.

Nolan, L., Wit, A., Dudzinski, K., Lees, A., Lake, M., Wychowanski, M., 2003. Adjustments in gait symmetry with walking speed in trans-femoral and trans-tibial amputees. Gait & Posture 17, 142–151.

Pandy, M.G., Lin, Y., Kim, H.J., 2010. Muscle coordination of mediolateral balance in normal walking. Journal of Biomechanics 43, 2055–2064.

Peterson, C.L., Hall, A.L., Kautz, S.A., Neptune, R.R., 2010. Pre-swing deficits in forward propulsion, swing initiation and power generation by individual muscles during hemiparetic walking. Journal of Biomechanics 43, 2348–2355.

Pinzur, M.S., Asselmeier, M., Smith, D., 1991. Dynamic electromyography in active and limited walking below-knee amputees. Orthopedics 14, 535–537.

Powers, C.M., Rao, S., Perry, J., 1998. Knee kinetics in trans-tibial amputee gait. Gait & Posture 8, 1–7.

Raasch, C.C., Zajac, F.E., Ma, B., Levine, W.S., 1997. Muscle coordination of maximum-speed pedaling. Journal of Biomechanics 30, 595–602.

Renstrom, P., Grimby, G., Larsson, E., 1983. Thigh muscle strength in below-knee amputees. Scandinavian Journal of Rehabilitation Medicine 9 (Supplement), 163–173.

Royer, T.D., Wasilewski, C.A., 2006. Hip and knee frontal plane moments in persons with unilateral, trans-tibial amputation. Gait & Posture 23, 303–306.

Sadeghi, H., Allard, P., Duhaime, P.M., 2001. Muscle power compensatory mechanisms in below-knee amputee gait. American Journal of Physical Medicine and Rehabilitation 80, 25–32.

Sanderson, D.J., Martin, P.E., 1997. Lower extremity kinematic and kinetic adaptations in unilateral below-knee amputees during walking. Gait & Posture 6, 126–136.

Silverman, A.K., Fey, N.P., Portillo, A., Walden, J.G., Bosker, G., Neptune, R.R., 2008. Compensatory mechanisms in below-knee amputee gait in response to increasing steady-state walking speeds. Gait & Posture 28, 602–609.

Torburn, L., Perry, J., Ayyappa, E., Shanfield, S.L., 1990. Below-knee amputee gait with dynamic elastic response prosthetic feet: a pilot study. Journal of Rehabilitation Research and Development 27, 369–384.

Underwood, H.A., Tokuno, C.D., Eng, J.J., 2004. A comparison of two prosthetic feet on the multi-joint and multi-plane kinetic gait compensations in individuals with a unilateral trans-tibial amputation. Clinical Biomechanics 19, 609–616.

Winter, D.A., Sienko, S.E., 1988. Biomechanics of below-knee amputee gait. Journal of Biomechanics 21, 361–367.

Winters, J.M., Stark, L., 1988. Estimated mechanical properties of synergistic muscles involved in movements of a variety of human joints. Journal of Biomechanics 21, 1027–1041.

Zajac, F.E., 1989. Muscle and tendon: properties, models, scaling, and application to biomechanics and motor control. Critical Reviews in Biomedical Engineering 17, 359–411.

Zajac, F.E., Neptune, R.R., Kautz, S.A., 2003. Biomechanics and muscle coordination of human walking: part II: lessons from dynamical simulations and clinical implications. Gait & Posture 17, 1–17.

Zmitrewicz, R.J., Neptune, R.R., Sasaki, K., 2007. Mechanical energetic contributions from individual muscles and elastic prosthetic feet during symmetric unilateral transtibial amputee walking: a theoretical study. Journal of Biomechanics 40, 1824–1831.